New Technologies for the High-Speed Characterization and Analysis of Essential Oils

by Tincuta Veriotti, Megan McGuigan and Richard Sacks, University of Michigan

Dramatic reductions in characterization and analysis times for essential oils were achieved using high-speed gas chromatography (HSGC) and time-of-flight mass spectrometry (TOFMS). High-speed separations were achieved with relatively short capillary separation columns operated with high carrier-gas flow rates and fast temperature programming. Unique features of TOFMS include high spectral acquisition rates and spectral continuity (constant ion-abundance ratios across chromatographic peak profile). These features allow for completely automated peak finding and spectral deconvolution of relatively narrow and severely overlapping chromatographic peaks from completely unknown mixtures. This reduces the chromatographic resolution requirements, and can result in order-of-magnitude reductions in the time required for mixture characterization. For HSGC analysis of characterized samples, selectivity is enhanced by the use of programmable carrier gas flow in a series-coupled ensemble consisting of a polar and a non-polar column. A valve connecting the column junction point to a ballast chamber containing carrier gas at the GC inlet pressure is used to stop the flow in the first column for short, programmed intervals in order to achieve greater separation of targeted component pairs that are separated by the first column in the ensemble, but co-elute from the ensemble. High-speed characterization and analysis of grapefruit oil is used to demonstrate these technologies. Using a temperature-programming rate of 50°C/min, complete characterization and analysis are achieved in less than 200 s.

> "The difficulties in (essential oil) analyses arise from the large number of components, many of them present at low concentrations . . ."

Essential oils are botanical substances widely used for their flavor and fragrance qualities. Hundreds of these oils are commercially available. Some of these natural products are highly valued as commodity and specialty materials for the flavor, fragrance and medicinal markets. The market value of these materials is strongly linked to composition, and adulteration in the service of enhanced profitability is not infrequent. Because many of these materials are used as flavorings and medicinal agents, health and safety issues are of concern.

For these reasons, the analytical chemistry of essential oils is very important, and the literature abounds with studies related to the characterization and quantitative analysis of these materials.[1,2] The difficulties in their analysis arise from the large number of components, many of them present at low concentrations, and large variations in composition with growing conditions, location and processing methods.[3] Since many of the constituents have structural similarities, characterization of the mixture components can be difficult. For example, essential oils contain many terpenes and oxygen-containing terpene structures. The oxygenated compounds are often responsible for the flavor and fragrance characters of specific oils. Terpenes can be rapidly oxidized by air with the development of unpleasant flavors and odors.[4]

Gas chromatography (GC) with flame ionization detection (FID) is often the method of choice for QA/QC analysis of essential oils. GC with mass spectrometry (MS) detection is most frequently used for the characterization of the components in these materials.[4-7] These methods are very slow, and limited sample throughput is a bottleneck in many applications. For complex mixtures, it is not always possible to obtain a complete separation using only one column, and analysis times of even 30 min to 60 min per sample may not obtain a complete separation.[2]

Much faster analysis can be obtained using relatively short capillary columns and fast temperature programming.[8-10] However, the resolving power of the column is substantially reduced resulting in more co-eluting mixture components.

 0272-2666/02/0009-0040$04.00/0—

In addition, most MS instruments cannot track the narrower chromatographic peaks. Different approaches have been attempted in order to solve these problems. These approaches include the use of columns with enhanced selectivity to cope with the reduced resolving power of shorter columns and time-of-flight (TOF) MS for characterization of the peaks from high-speed separations.

TOFMS: Most mass spectrometers used for the characterization of complex mixtures scan the mass spectrum over a sufficiently large mass range to identify all target compounds in the mixture. Often electron ionization (EI) is used to generate an ion fragmentation pattern for each chromatographic peak, and the peak is identified by means of a library search. As the mass (m/z) is scanned, the ion currents from the different mass fragments are measured sequentially. Typical scan rates are about one Da/ms; maximum spectral acquisition rates are typically less than a few spectra per s.[11,12]

This has two important implications. First, since each mass fragment is monitored for only a relatively small fraction of the total scan-time, signal-to-noise ratios are often smaller than for selected-ion monitoring (SIM), in which a single m/z is monitored for the entire measurement interval.[13] Second, the sample vapor pressure in the ion source changes during a scan due to the evolution of the chromatographic peak. This results in a skewing of the mass spectra, which depends on the change in vapor pressure during the scan. Spectral skewing reduces the reliability of peak identification by comparison of the fragmentation pattern with spectral libraries. In order to minimize the effects of spectral skewing and to collect sufficient spectra for the characterization of every chromatographic peak, slow separations producing relatively broad peaks usually are used. This is incompatible with fast separations, which produce narrow peaks.

Time-of-flight MS completely eliminates spectral skewing and can achieve very high spectral acquisition rates. The right-hand portion of Figure 1 illustrates the concept. The GC effluent is introduced directly into an EI source, and narrow pulses of ions are extracted from the source at a frequency of several kHz. Each pulse contains ions of all m/z values generated in the GC effluent vapor. Each ion pulse enters a field-free drift tube, is reflected off of an electrostatic ion mirror and strikes a sensitive detector.

Ions of smaller m/z in each pulse travel faster in the drift tube than ions of larger m/z, and the former reach the detector before the latter. Thus, ions of different m/z are dispersed in time at the ion detector.[14] Typically, the ion currents are measured for several hundred m/z values, which span the range necessary for the complete characterization of the mixture. In order to increase signal-to-noise ratios, the ion currents are averaged over a number of pulses. For the instrument used here (Pegasus II, LECO, St. Joseph, MI), 5,000 pulses are generated per s, and 10 or more are averaged for each display point in the extracted-ion chromatograms. This gives a maximum spectral acquisition rate of 500 full-mass-range spectra per second.[15,16]

Figure 1. Schematic of the TOFMS and high-speed GC with stop-flow selectivity enhancement; see text for component descriptions

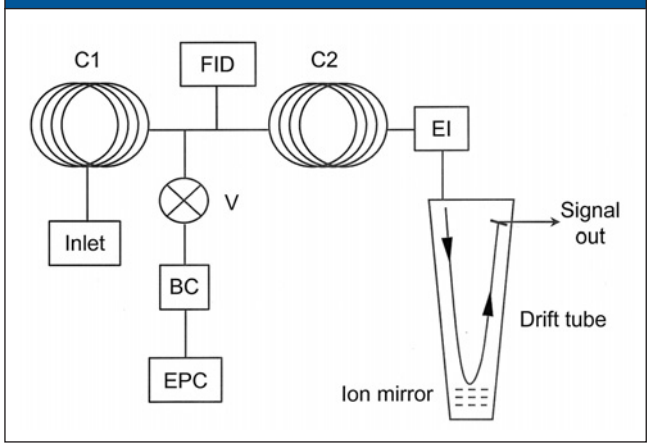

Figure 2. Benzene peak showing mass spectra at different points on the peak profile

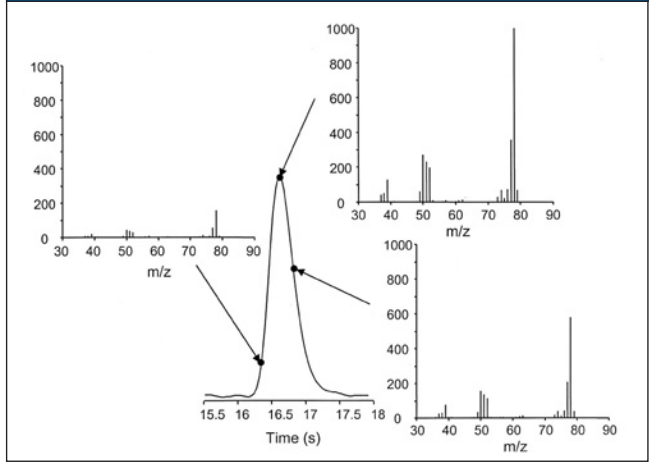

In addition to high spectral acquisition rates, which allow tracking very narrow chromatographic peaks, TOFMS produces constant ion-abundance ratios across the chromatographic peak profile (no spectral skewing). This is illustrated in Figure 2 for a benzene peak. Note that the full peak width at half height is only 0.33 s. The mass spectra for three representative points on the chromatographic peak are also shown in Figure 2. Note that the ion-abundance ratios are nearly identical in the three spectra.

If the ion-abundance ratios change across the chromatographic peak profile, chromatographically unresolved peaks are indicated; instrument software can find the apexes of the individual peaks and deconvolute the spectra, resulting in spectra for the individual components. These deconvoluted spectra can then be matched to library spectra for component identification. The ability of the TOFMS system to characterize components in severely overlapping chromatographic peaks — provided that the mass spectra

for the components are sufficiently different — can dramatically reduce the resolution requirements for the GC.

GC selectivity enhancement: For QA/QC applications, GC with FID detection is typically used; all target compounds must be adequately resolved for quantitative measurements. If short columns are used for high-speed analysis, enhanced GC selectivity is required to cope with reduced resolving power. The left-hand side of Figure 1 shows a GC instrument designed for programmable selectivity. Two capillary GC columns (C1 and C2) using different stationary phases are connected in series so that all mixture components migrate through both columns prior to detection with an FID or MS. A second FID connected to the column junction point is used to monitor a small fraction of the effluent from the first column. The column junction point is also connected to a ballast chamber (BC) through valve (V). An electronic pressure controller (EPC) is used to set the ballast chamber pressure equal to the GC inlet pressure.

For two columns connected in series, a change in the pressure at the column junction-point will increase the carrier-gas flow in one of the columns and decrease the flow in the other column. If the pressure change is implemented for a short period of time (pressure pulse), column ensemble selectivity can be adjusted to increase the separation of a specific peak pair without significant effect on the retention pattern for the rest of the peaks in the chromatogram.[17,18] When a complex mixture is injected into a tandem-column ensemble, many components will be separated in the first column, and stay separated in the second column. Other components, which are not separated in the first column, will be separated in the second column. For components that are not separated by either column, no amount of coaxing will result in their separation by the column ensemble. What is of interest in this report is the frequent situation in which components are separated in the first column, but co-elute from the column ensemble by virtue of the different selectivites of the columns for those components.

If the ballast chamber pressure in Figure 1 is set equal to the GC inlet pressure, then the carrier-gas flow in C1 completely stops when the valve is open (stop-flow operation), and the flow in C2 significantly increases. For component pairs that are separated in the first column but co-elute from the column ensemble, the valve is opened for a few seconds when one of the targeted components has crossed the junction point, and is in the second column, yet the other component is still in the first column. This delays the elution from the ensemble of the component that was in C1 when the valve was opened, and results in the ensemble separation of the targeted pair. For component pairs that are in the same column when the valve is opened, there will be only small changes in their separation.

The stop-flow concept is illustrated in Figure 3, which shows plots of the migrating sample bands along the column ensemble axis versus time for four target compounds.

Figure 3. Enhanced selectivity by stopping the carrier gas flow in the first column; (a), no stop-flow pulse; (b), one stop-flow pulse to enhance the separation of component pair A/B; (c) two stop-flow pulses to enhance the separation of component pairs A/B and C/D

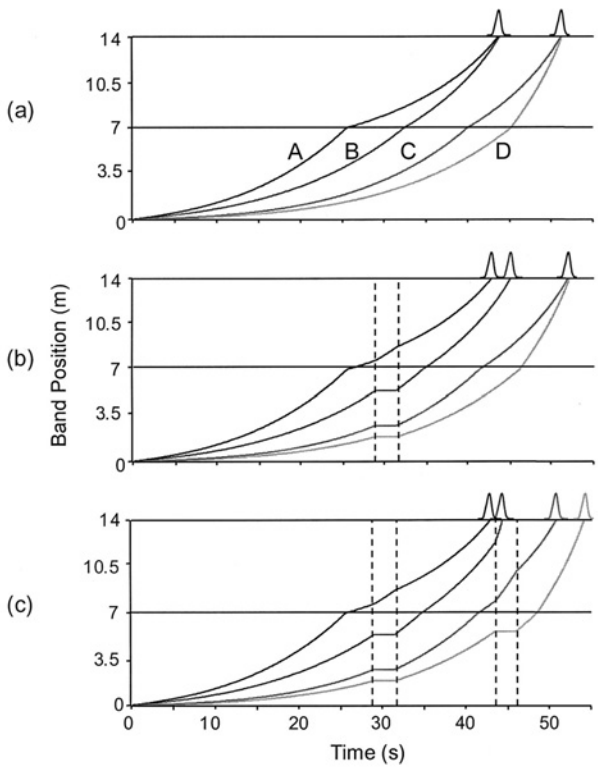

The local slopes of these plots give the band migration velocities at the corresponding positions along the column axis. The plots are for the case of a temperature-programmed separation using a linear temperature ramp of 50°C/min. The lower left corner of each set of plots corresponds to sample injection, and the upper horizontal line at 14 m (column ensemble length) corresponds to elution from the ensemble. The horizontal line at 7 m corresponds to the column junction point. Note in Figure 3(a) that the plots for the different compounds show discontinuities across the column junction point. This is the result of the different selectivities of the two columns. The curvature in the plots is the result of the increase in band migration rates with increasing column temperature during the temperature program and the acceleration of the carrier gas due to decompression from the ensemble inlet to the outlet.

The compounds used for this example are all well separated by the first column, but elute from the column ensemble as two co-eluting pairs. The peaks shown above the plots in Figure 3(a) indicate these pairs. For the plots in Figure 3(b), the valve in Figure 1 was opened for 2.5 s beginning 29 s after injection. Component A eluted from the first column in about 25 s, and thus was in the second column when the valve was opened. This band accelerated when the valve was open; its ensemble retention time was

shifted to a slightly smaller value. The other three bands were in the first column when the valve was opened, and completely stopped until the valve was closed. This resulted in a substantial increase in their ensemble retention times. The result is the complete separation of components A and B in the ensemble chromatogram. As shown in Figure 3(c), the valve can be opened a second time about 43 s after injection when component C is in the second column, but component D is still in the first column. The result is the complete separation of the mixture.

Instrumentation, Methods and Materials

The basic instrument consists of an HP6890 GC (Hewlett-Packard, Atlanta, GA) equipped with an FID, a split-splitless inlet operated in the split mode, an HP7683 auto-injector and a Pegasus II TOFMS (LECO Corp., St Joseph, MI). For this study, a 14-m long column ensemble was used, consisting of 7.0 m of moderately polar trifluoropropylmethyl polysiloxane (DB-200, J&W Scientific, Folsom, CA) followed by 7.0 m of non-polar 5% phenyl dimethlypolysiloxane (DB-5, J&W Scientific). Both columns were 0.18-mm i.d., and used 0.20-mm thick-bonded stationary phases. Hydrogen was used as carrier gas at an inlet temperature of 250°C and an inlet pressure of 35.0 psig. An initial temperature of 50°C and a temperature-programming rate of 50°C/min beginning at the time of injection were used.

Figure 4. High-speed chromatogram of grapefruit oil using TOFMS detection with the display showing the sum of m/z 82 and 134; the inset shows the congested region indicated in the broken-line box; peak numbers correspond to the component numbers in Table 1

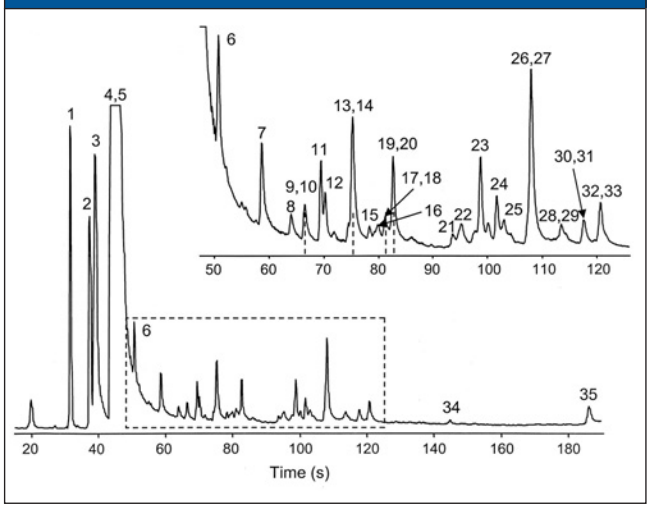

The TOFMS instrument was operated with EI at 70 eV. A spectral acquisition rate of 25 spectra/s was used. The user-defined signal-to-noise (S/N) threshold was set to find all peaks with S/N>100. Manufacturer's software was used for automated peak finding and deconvolution. Characterization of found peaks was accomplished by means of a small (about 70 components) TOFMS library developed for this project, which contained some of the most frequently encountered essential oil components, and a commercial terpene library containing more than 1,200 entries. One peak was identified with the NIST MS database. The Pegasus II software was used for all instrument control functions and for spectral data acquisition.

For studies of enhanced selectivity using stop-flow operation of the first column, a low-dead-volume, pneumatically-operated valve was used (Model MOPV-1/50, SGE, Austin, TX) to connect the column junction point to a 300-mL ballast chamber. The ballast chamber pressure was set equal to the GC inlet pressure by means of a high-precision pressure controller (Model 640A, MKS Instruments, Andover, MA).

Grapefruit oil (Gritman Essential Oils, Friendswood, TX) was used to illustrate the utility of the TOFMS and stop-flow operation for high-speed characterization and analysis. Because a wide range of analyte concentrations is present in the sample, dilutions in acetone were used to prepare analytical curves (deconvolued total-ion peak area vs. concentration). These plots were used to compute the percent of the total peak area for each analyte. For all studies, 0.20-µL injections were used with a split ratio of 150:1.

High-Speed Characterization and Analysis of Grapefruit Oil

While the other citrus oils have been studied extensively, relatively few data are available for grapefruit (Citrus paradisi). Guenther reported one of the earliest investigations of grapefruit oil in 1949. Kirchner and Miller followed in 1953 with a more extensive study of the volatile components. MacLeod and Buigues confirmed the presence of nootkatone, a sesquiterpene ketone that is believed responsible for the distinctive aroma and flavor of grapefruit oil.[19-21] More recently, Pino and Sanchez used GC/MS to identify and obtain quantitative analysis of 24 components in cold-pressed grapefruit oil and grapefruit-oil concentrates.[4]

TOFMS characterization of grapefruit oil: Data from the TOFMS (sum of m/z 82 and 134) are presented in Figure 4. Thirty-five components of grapefruit oil elute from the column in a little more than 3 min. The chromatogram from the ensemble is very complex and congested. Most of the major constituents eluted in the first 50 s, with limonene (peak 4) being the most abundant component. The other region contains components present at lower concentrations, and is presented as an inset in Figure 4. The last component of interest (nootkatone, peak 35) eluted in just over 3 min.

Careful inspection of extracted-ion chromatograms showed that all peaks for analytes with S/N values above the threshold (100:1) were found with the peak-finding software, and overlapping peaks were successfully deconvoluted. Table 1 lists the compounds identified in the grapefruit oil. Peak numbers correspond to Figure 4. Similarities for library matches are also included. Of the 35 found peaks, 20 were identified from the TOFMS library, which confirms component identification by retention index as well as by the mass spectra. For these peaks, average similarity was 914. Ten peaks were identified from the terpene library with an average similarity of 864. One peak was identified with the NIST MS database. For peaks 16, 19, 24 and 25, similarities were too poor for positive peak identification.

Examples of the extracted-ion chromatograms for some overlapping peaks are shown in Figure 5. The total-ion-current chromatograms for the regions extending from 66 s to 76 s, and from 114 s to 124 s, are shown in Figures 5(a) and 5(c), respectively. The corresponding extracted-ion chromatograms for several m/z are shown in Figures 5(b) and 5(d), respectively. Vertical lines indicate the retention times of the found peaks. The numbers next to the vertical lines correspond to the component numbers in Table 1. The numbers with arrows pointing to the various extracted-ion chromatograms give the m/z values. Note that for peak pairs 30/31 and 32/33, the peak apex separations are only 0.20 s and 0.16 s, respectively. Despite the severe overlap of these peak pairs, automated peak finding, spectral deconvolution and component identification were successful.

Calibration plots (log peak area vs. log concentration) for several of the mixture components from MS measurements are shown in Figure 6. Plot numbers refer to component numbers in Table 1. Statistical data for these plots is presented in Table 2. Correlation coefficients range from 0.990 to 0.9994. Log-log slopes range from 0.87 to 1.12. Perfect response linearity with concentration should give a log-log slope of 1.00. From these calibration plots, the percent of total peak area for each component was computed. Values are given in Table 1.

Figure 5. Total-ion chromatograms (a) and (c) and extracted ion chromatograms (b) and (d) for two regions in the high-speed chromatogram of grapefruit oil; vertical lines show retention times assigned by the automated peak-finding algorithm; peak numbers correspond to component numbers in Table 1; numbers by the extracted-ion chromatograms give the m/z values

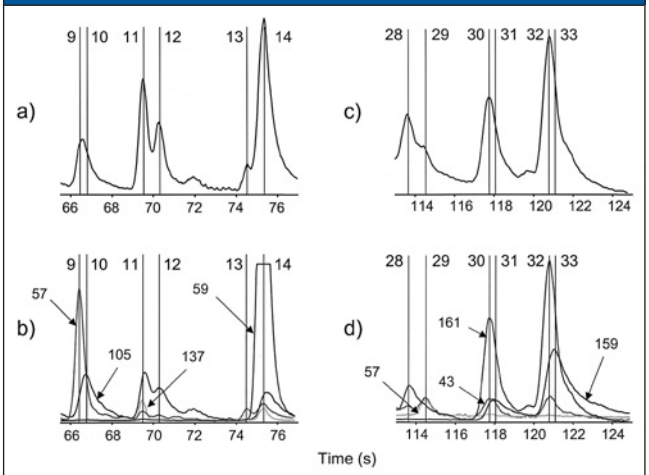

Figure 6. Plots of log (peak area) versus log (concentration) for some components in grapefruit oil; plot numbers correspond to component numbers in Table 1

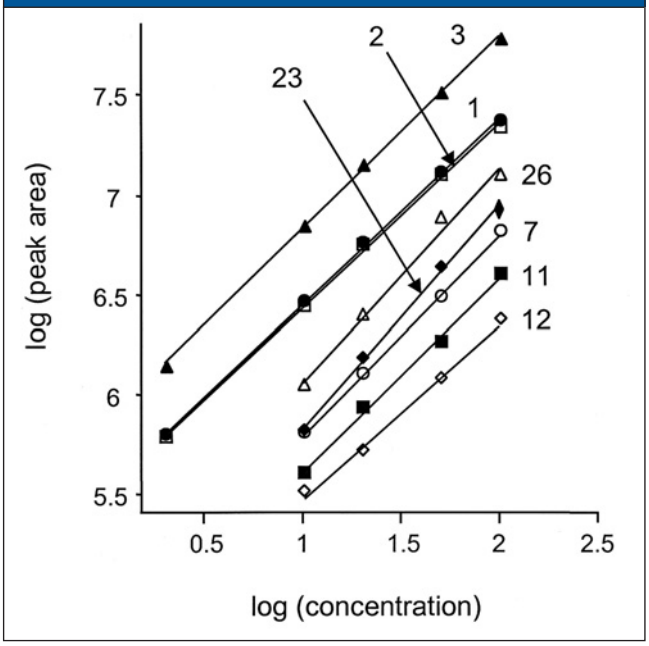

Enhanced GC selectivity for grapefruit oil: The FID that monitors a fraction of the effluent from column C1 (see Figure 1) is helpful in determining the valve opening times required for the enhanced separation of targeted peak pairs. However, once a method is developed, this detector is not needed. Figure 7 shows the FID chromatogram for the grapefruit oil. Note that this chromatogram is from the first column only, and thus is lower resolution than the chromatogram from the column ensemble.

In the ensemble chromatogram (Figure 4), component pairs 9/10, 13/14, 17/18 and 19/20 all co-elute, but all four pairs are separated in the FID chromatogram of Figure 7. The broken vertical lines in the inset of Figure 7 indicate points in the FID chromatogram where opening the valve will enhance the separation of the different component pairs. It is not necessary that the FID peaks for a targeted component pair be isolated by the first column. For example, components 13 and 14 are completely separated by the first column, but 13 co-elutes with 15 and 16. This is of no concern since 13, 15 and 16 are all separated by the second column, and thus are separated in the ensemble chromatogram.

Figure 8 shows the enhanced separation achieved for this portion of the ensemble chromatogram by using a sequence of four stop-flow pulses. If a 2-s stop-flow pulse is applied beginning 49.5 s after injection (see Figure 7), components 1 through 9 are already in the second column; the increase in flow in this column results in small shifts to shorter retention times. The rest of the components are stopped in the first column for the entire pulse duration. Since components 9 and 10 are in different columns during the stop-flow intervals, the change in pressure will affect them in different ways; an increase in their separation is achieved both at the end of the first column and at the end of the column ensemble. Figures 8(a) and 8(b) compare the ensemble chromatograms (sum of m/z 82 and 134) without and with a 2-s pulse, respectively. The arrows indicate the changes in retention times for peaks 9 and 10. Note that peaks 10-20, which were all in column C1 when the valve was opened, are all shifted to greater retention times, yet the pattern of peaks has not changed significantly.

Because components 13 and 14 were also well separated on the first column, a sequence of two 2-s pulses applied at 49.5 s and 59.3 s after injection resulted in an increase in separation for both pairs 9/10 and 13/14 [Figure 8(c)]. Note that the application of the second pulse is delayed compared with the FID retention times from Figure 7, since the application of the first pulse delays all the components present in C1 for the pulse duration.

Three pulses applied at 49.5 s, 59.3 s and 66.8 s after injection resulted in complete separation of an additional pair [17/18; Figure 8(d)]. Again, the last pulse of the sequence was delayed because of the increase in retention time on the first column caused by both the first and the second pulses in the sequence. As shown by Figure 8(e), the addition of a fourth pulse to the sequence at 71.8 s after injection, which targeted component pair 19/20, resulted in adequate separation of almost all peaks in this region of the chromatogram. More co-elutions are present in the last part of the ensemble chromatogram (Figure 4), but none of the pairs are completely separated by the first column.

Table 1. Grapefruit Oil Composition

Peak #	Compound Name	Similarity	% Area
1	α-pinene[a]	944	1.37
2	β-pinene[a]	884	1.27
3	myrcene[a]	949	3.57
4	limonene[a]	945	89.31
5	2-carene[a]	893	0.16
6	octanal[a]	932	0.23
7	linalool[a]	938	0.37
8	verbenene[b]	877	<0.1
9	3-carene-2-ol[b]	857	<0.1
10	nonanal[a]	845	<0.1
11	perilla alcohol	860	0.23
12	limonene oxide[a]	962	0.14
13	α-terpineol[a]	921	0.23
14	dihydrocarveol[a]	868	<0.1
15	nerol[a]	892	<0.1
16			<0.1
17	carveol[a]	934	<0.1
18	acetic acid, octyl ester	857	<0.1
19			<0.1
20	decanal[a]	930	0.18
21	neral[a]	873	<0.1
22	carvone[a]	952	<0.1
23	geranial[a]	869	0.51
24			0.22
25			<0.1
26	β-caryophyllene[a]	967	0.73
27	geranyl acetate[a]	928	0.15
28	ocimene isomer[b]	861	<0.1
29	humulene[b]	866	<0.1
30	germacrene D[b]	842	<0.1
31	cadinene isomer[b]	875	<0.1
32	cadinene isomer[b]	882	0.2
33	calamene isomer[b]	875	<0.1
34	himachalene[b]	842	<0.1
35	nootkatone[a]	847	0.14

[a]compounds identified with TOF library
[b]compounds identified with terpenes library

Conclusions

The important attributes of TOFMS for the high-speed characterization of essential oils include high signal-to-noise ratios, high spectral acquisition rates and the absence of spectral skewing. With these features, software can be used for the automated finding and deconvoluting of se-

Figure 7. Grapefruit-oil chromatogram from the FID monitoring the effluent from the first column

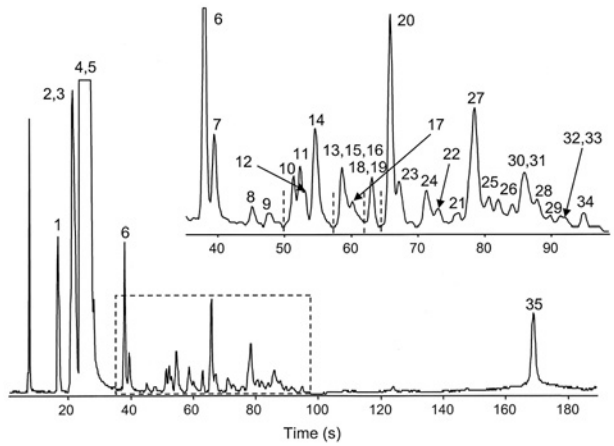

Figure 8. Enhanced selectivity for grapefruit-oil components; (a) no stop-flow pulses; (b) one stop-flow pulse to separate peak pair 9/10; (c) two stop-flow pulses to separate peak pairs 9/10 and 13/14; (d) three stop-flow pulses to separate peak pairs 9/10, 13/14 and 17/18; (e) four stop-flow pulses to separate peak pairs 9/10, 13/14, 17/18 and 19/20

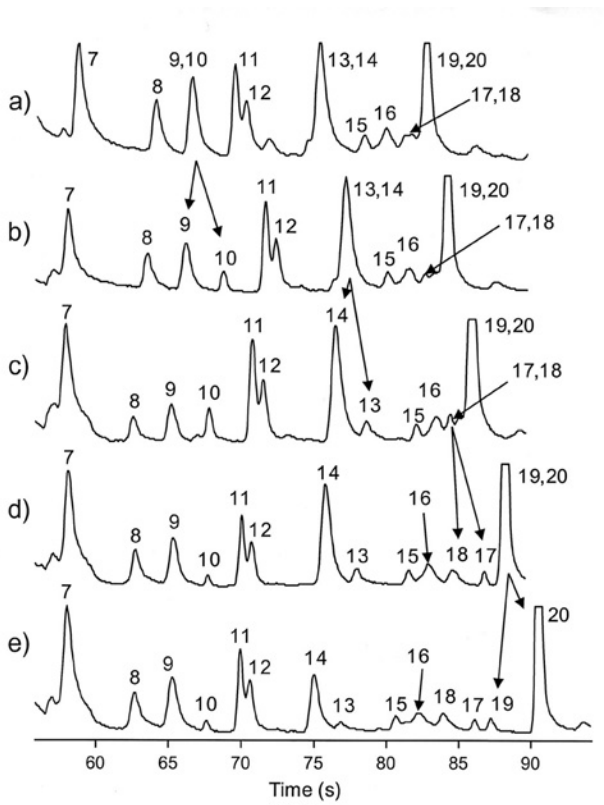

verely overlapping peaks for completely unknown mixtures. When combined with high-speed GC, 35 components present in grapefruit oil are characterized in a little over 3 min. Automated peak finding and deconvolution at an acquisition rate of 25 spectra/s and a signal to noise ratio of 100:1 were successful for all of the components.

A unique aspect of the stop-flow technology is the ability to target specific peak pairs for enhanced separation and enhanced resolution without significantly changing the resolution of other adjacent peak pairs. The stop-flow pulse method is useful in enhancing the separation of complex mixtures, if the condition of complete separation at the end of the first column is satisfied.

High-speed GC is achieved by using short columns and high carrier-gas flow rates. This approach trades resolution for speed. The problems associated with reduced resolution and peak capacity are addressed by the use of the technologies described in this article by increasing selec-

tivity using stop-flow column methods or by reducing resolution requirements using TOFMS. The conditions used here were chosen to obtain very fast separation and characterization. By using long, higher resolution columns, relatively fast mixture separation and characterization can be achieved with reduced reliance on programmable column selectivity and peak deconvolution with TOFMS.

Acknowledgements

The authors gratefully acknowledge LECO Corp., St. Joseph, MI for the use of the time-of-flight mass spectrometer (Pegasus II), and Gritman Essential Oils, Friendswood, TX for providing the grapefruit oil sample used for this study.

Address correspondence to Richard Sacks, Department of Chemistry, University of Michigan, Ann Arbor, MI 48109

References

1. V. Formaceck and K. Kubeczka, *Essential Oils Analysis by Capillary Gas Chromatography and C-13 NMR Spectroscopy*, Wiley: New York, (1982).
2. Y. Masada, *Analysis of Essential Oils by Gas Chromatography and Mass Spectrometry*, Wiley: New York (1976).
3. F. Millet, M. Monghal, M. Rollet and J. Dorche, Ann. Pharm. Fr., 28, 63 (1970).
4. J. Pino and M. Sanchez, J. Essent. Oil Res., 12, 167 (2000).
5. D. Sun and P. Petracek, J. Agric. Food Chem., 47, 2067 (1999).
6. P. Stremple, J. High Resol. Chromatogr., 21, 587 (1998).
7. G. Cartoni, G. Goretti, B. Monticelli and M. Russo, J. Chromatogr., 370, 93 1986).
8. J. Davis and J. Giddings, Anal. Chem., 55, 418 (1983).
9. E. Ehrmann, H. Dharmasena, K. Carney and E. Overton, J. Chromatogr. Sci., 34, 553 (1996).
10. A. Grall, C. Leonard and R. Sacks, Anal. Chem., 72, 591 (2000).
11. E. Schlag, *Time of Flight Mass Spectrometry and its Applications*, Elsevier: New York (1994).
12. R. Cotter, *Time of Flight Mass Spectrometry*, American Chemical Society: Washington, DC (1994).
13. C. Sweeley, W. Elliott, I. Fries and R. Ryhage, Anal. Chem., 38, 1549 (1966).
14. E. Erickson, C. Enke, J. Holland and J. Watson, Anal. Chem., 62, 1079 (1990).
15. M. van Deursen, H. Janssen and C. Cramers, *Proceedings of the 21st International Symposium on Capillary Chromatography and Electrophoresis*, Park City, UT, June 20-24, p. 186 (1999).
16. C. Leonard and R. Sacks, Anal Chem., 71, 5177 (1999).
17. T. Veriotti and R. Sacks, Anal. Chem., 73, 3045 (2001).
18. T. Veriotti and R. Sacks, Anal. Chem., 73, 4395 (2001).
19. E. Guenther, *Essential Oils of the Genus Citrus*, In: *The Essential Oils*, Vol. III, pp 347-357, Van Nostrand, New York (1949).
20. J. Kirchner and J. Miller, J. Agr. Food Chem. 1, 512 (1953).
21. W. MacLeod and M. Buigues, J. Food Sci., 29, 565 (1964). ■